

Basic Molecular Mechanisms Underlying Complex Permittivity of Water and Ice

Vladimir I. Gaiduk*[†] and Derrick S. F. Crothers[‡]

Institute of Radio Engineering and Electronics of the Russian Academy of Sciences, Vvedensky Sq. 1, Fryazino, 141190, Moscow Region, Russia, and Queen's University Belfast, Belfast BT7 INN, Northern Ireland

Received: February 1, 2006

Four dielectric-loss frequency dependences $\epsilon''_j(\nu)$, $j = 1-4$, which constitute a basis for underlying far-infrared (FIR) spectra of water and ice, are briefly analyzed. The relevant molecular mechanisms are (a) free-like libration of a permanent dipole in a hat potential, (b) elastic vibration of a nonrigid dipole along the H-bond (HB), (c) elastic reorientation of a permanent dipole around this bond, and (d) vibration of HB water molecules transverse to the HB direction. A semiphenomenological (SP) approach, based on analytical calculation of the spectrum of autocorrelation function, is applied. The total loss curve $\epsilon''(\nu)$, accounting for these mechanisms and presented for liquid water at 27 and 81.4 °C, for supercooled water at -5.6 °C, and for ice at -7 °C, demonstrates a very good agreement with experimental spectra. A simple formula is proposed for an "association factor" ζ relating the dipole moments μ_\perp and μ_q of transversally and longitudinally (with respect to HB direction) vibrating molecules. The parametrization of the model yields for $T < 300$ K a sharp increase of this factor ζ with a decrease of temperature.

Introduction

Understanding of molecular mechanisms, governing complex permittivity $\epsilon(\nu)$ of water and ice, is of a fundamental interest and of practical importance, the "frequency" ν being, as usual, the wavenumber, whereas $\epsilon \equiv \epsilon' + i\epsilon''$ (the complex-conjugation symbol is omitted).

Theoretical $\epsilon(\nu)$ spectra of water could be obtained by the molecular-dynamics (MD) simulation method; see, e.g., refs 1–7 and references therein. The MD method, which represents a computational experiment, is based on consideration of pair interactions in a large assembly of water molecules. However, this method is complex, characterized by high cost of computation and difficulty in calculation of the low-frequency permittivity $\epsilon(\nu)$. Up to now the MD method yields only a *qualitative* agreement with experiment. These drawbacks are avoided in the semiphenomenological (SP) approach,^{8–10} in which the one-particle approximation is used and the effective potentials, governing motion of rigid or nonrigid dipoles, are introduced on an *intuitive* basis. Being less fundamental for this reason, than the MD method, the SP approach obtains, however, a good *analytical* description of the experimental $\epsilon(\nu)$ dependences.

We demonstrate in this communication that the main features of the complex permittivity $\epsilon(\nu)$ pertinent to water and ice may be properly described, if *four* molecular mechanisms (a), (b), (c), (d) are involved on the basis of a semiphenomenological modeling of spectra in terms of classical theory. The first mechanism (a) refers to dielectric relaxation pertinent to a permanent dipole influenced by a rather narrow hat intermolecular potential, the next two (b, c) refer to the complex permittivity generated by two elastically vibrating hydrogen-bonded (HB) molecules. The last mechanism (d) refers to a nonrigid dipole vibrating in direction perpendicular to that of the undisturbed H-bond. Mechanism a is described in refs 10–12, mechanisms b and c in ref 13, and mechanism d in ref 14.

In this correspondence our recent theory of complex permittivity pertinent to mechanism d is considered and application¹⁵ of this theory for water in a range of temperatures is briefly observed. We place emphasis just on a specific role of the d mechanism in formation of far-IR spectra of water and ice. We shall consider the wideband spectrum of water in the range 0–1000 cm^{-1} and the spectrum of ice in the far-infrared (FIR) range 10–1000 cm^{-1} applying the two-fractional (mixed) SP model, in which one fraction refers to the librational (LIB) and the other to the vibrational (VIB) modes of molecular motion.

First, we shall illustrate the loss spectra relevant to each of the four specific mechanisms (we term "loss" the imaginary part of ϵ). At the end of our communication we shall demonstrate the total loss spectrum by taking into account all mechanisms. The employed molecular constants and the fitted and estimated model parameters are given in Table 1.

Mechanism a: Loss Contribution ϵ''_{or} of a Librating Permanent Dipole.^{10–13} This mechanism refers to the *LIB state* and concerns quasi-resonance dielectric response generating the librational band located near the border of the infrared region (at $\nu_{\text{or}} \approx 700$ and ≈ 900 cm^{-1} , respectively, in water and ice). In terms of our SP approach the far-IR band arises from a rather free reorientation of a permanent dipole μ in the hat-like potential well typical of broken or strongly bent hydrogen bonds. In the low-frequency limit the mechanism a *formally* (after a proper parametrization) also describes the nonresonance Debye relaxation band, whose loss peak is located at microwaves. A useful molecular interpretation of this band was given for *water*, e.g., in ref 16, whereas in ref 17 a convenient empirical formula for $\epsilon(\nu)$ was proposed. For *ice* a similar nonresonance band is located at extremely low frequencies (in the kilohertz region). An empirical description of $\epsilon(\nu)$ in this region is known (see ref 18 and references therein); however, it appears that a relevant molecular interpretation of this band is lacking. The relaxation band of ice is not considered here.

The lifetime τ_{or} of the LIB state is commensurable with a part of a picosecond; in ice τ_{or} is several times shorter than in

[†] Institute of Radio Engineering and Electronics of the Russian Academy of Sciences. E-mail: vigaiduk@mail.ru.

[‡] Queen's University Belfast. E-mail: d.crothers@qub.ac.uk.

TABLE 1: Fitted and Estimated Parameters of the Molecular Model^a

water at 81.4 °C	$\epsilon_s = 61.8$ $\beta = 23.8^\circ$ $k_{ } = 14\,560$ dyne cm ⁻¹ $k_{\perp} = 4370$ dyne cm ⁻¹	$\rho = 0.971$ g cm ⁻³ $f = 0.9$	$\tau_D = 3.17$ ps $\tau_{or} = 0.08$ ps $\tau_q = 0.076$ ps $\tau_{\perp} = 0.064$ ps	$n_{\infty}^2 = 1.7$ $u = 6.8$ $\nu_q = 165$ cm ⁻¹ $p_{\perp} = 0.4$	$r_{or} = 65\%$ $\mu_q = 5.3$ D $g_{\perp} = 8.4$	$k_{\mu} = 1.19$ $\mu_{\mu} = 7$ D $m_{\perp} = 0.083$	$\mu_{or} = 2.7$ D $c_{rot} = 0.12$	$m_{or} = 1.5$
water at 27 °C	$\epsilon_s = 77.6$ $\beta = 23^\circ$ $k_{ } = 14\,560$ dyne cm ⁻¹ $k_{\perp} = 4370$ dyne cm ⁻¹	$\rho = 0.996$ g cm ⁻³ $f = 0.8$	$\tau_D = 7.85$ ps $\tau_{or} = 0.12$ ps $\tau_q = 0.076$ ps $\tau_{\perp} = 0.1$ ps	$n_{\infty}^2 = 1.7$ $u = 8.0$ $\nu_q = 165$ cm ⁻¹ $p_{\perp} = 0.65$	$r_{or} = 65\%$ $\mu_q = 7.0$ D $g_{\perp} = 3.9$	$k_{\mu} = 1.08$ $\mu_{\mu} = 6.35$ D $m_{\perp} = 0.071$	$\mu_{or} = 2.45$ D $c_{rot} = 0.12$	$m_{or} = 2.3$
supercooled water at -5.6 °C	$\epsilon_s = 90.2$ $\beta = 21.5^\circ$ $k_{ } = 16\,380$ dyne cm ⁻¹ $k_{\perp} = 6740$ dyne cm ⁻¹	$\rho = 0.999$ g cm ⁻³ $f = 0.7$	$\tau_D = 22.4$ ps $\tau_{or} = 0.28$ ps $\tau_q = 0.08$ ps $\tau_{\perp} = 0.2$ ps	$n_{\infty}^2 = 1.7$ $u = 8.5$ $\nu_q = 175$ cm ⁻¹ $p_{\perp} = 4.5$	$r_{or} = 65\%$ $\mu_q = 6.15$ D $g_{\perp} = 154$	$k_{\mu} = 1.08$ $\mu_{\mu} = 6.0$ D $m_{\perp} = 0.028$	$\mu_{or} = 2.45$ D $c_{rot} = 0.12$	$m_{or} = 5.6$
ice at -7 °C	$\epsilon_s = 94$ $\beta = 23.5^\circ$ $k_{ } = 22\,480$ dyne cm ⁻¹ $k_{\perp} = 6740$ dyne cm ⁻¹	$\rho = 0.92$ g cm ⁻³ $f = 0.15$	$\delta_{\infty} = 1.9$ $\tau_{or} = 0.06$ ps $\tau_q = 0.23$ ps $\tau_{\perp} = 0.03$ ps	$u = 8.5$ $\nu_q = 205$ cm ⁻¹ $p_{\perp} = 0.4$	$r_{or} = 70\%$ $\mu_q = 7.0$ D $g_{\perp} = 7$	$k_{\mu} = 1.06$ $\mu_{\mu} = 4.4$ D $m_{\perp} = 1.31$	$\mu_{or} = 1.9$ D $c_{rot} = 0.16$	$m_{or} = 2.1$

^a The employed molecular constants are $M = 18$, $I_{or} = 1.483 \times 10^{-40}$ g cm², $I_{vib} = 3.38 \times 10^{-40}$ g cm², $\mu_0 = 1.84$ D, $s_{lim} = 0.2$.

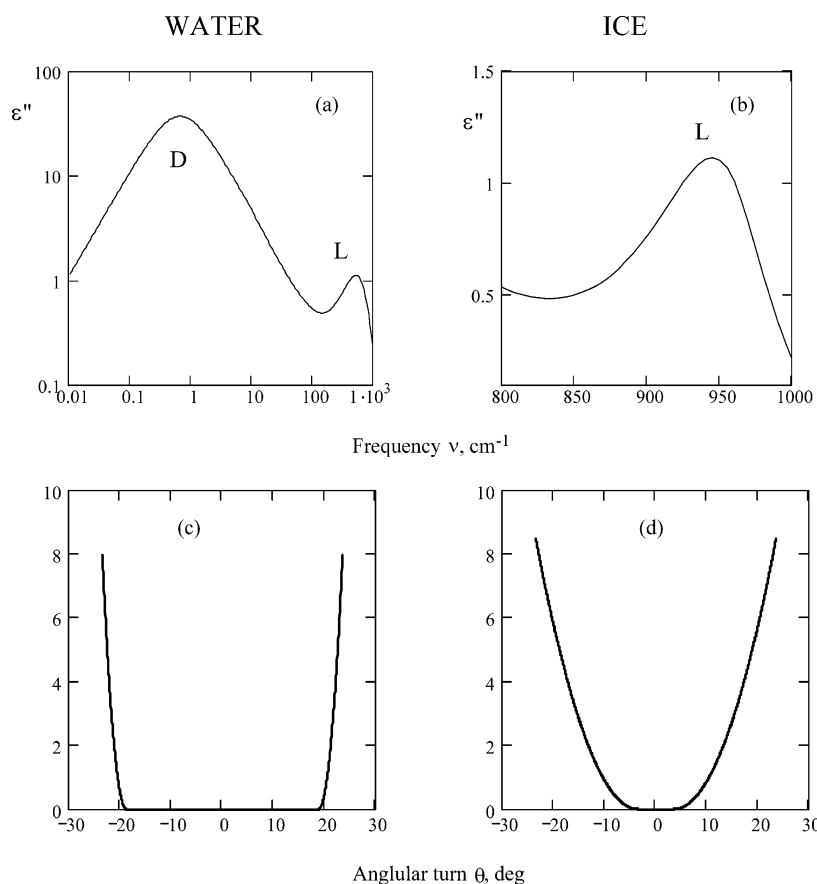


Figure 1. Dielectric-loss spectrum pertinent to libration of a permanent dipole in the hat well (a) and profile $U(\theta) (k_B T)^{-1}$ of such a well (c); calculation for water at 27 °C. Loss spectrum (b) and profile of the hat well (d) calculated for ice at -7 °C. Symbols D and L refer respectively to the Debye relaxational and librational bands.

water (see Table 1). An important feature of this state is fast chaotic reorientation (sometimes termed *disorder*) of hydrogen atoms inside a rather stable tetrahedral-like network of oxygen atoms. This reorientation is *cooperative*,¹² because a rotating proton, attached to a water molecule, jumps in a certain “favorable” configuration to form another H-bond.^{19,20} The libration of dipoles in the hat well is perhaps more chaotic in ice than in water, because $\tau_{or}(\text{ice}) \ll \tau_{or}(\text{water})$. A close connection between motions of hydrogen atoms and dielectric properties of aqueous fluids reveals itself in a great difference in the values of static dielectric permittivity ϵ_s of ice I_h and ice II. In ice I_h, where the proton disorder is emphasized, ϵ_s is as

high as ≈ 100 , whereas in ice II, where such a disorder is lacking, the static dielectric permittivity is low²¹ ($\epsilon_s \approx 3.66$).

The profile of the hat well is characterized by the libration amplitude β , by the normalized (divided by $k_B T$) well depth u , and by the form factor f determined as the ratio $f = (\text{potential width near the bottom})/(\text{potential width near the edge of the well})$.

The adopted well has parabolic walls and a flat bottom (see Figure 1c,d). The well is rather deep (u is about 8), whereas the well width 2β is about 45°. Unlike the well width 2β and the well depth $U_{or} \equiv uk_B T$, the parameter f strongly depends on the structure of the fluid and the temperature. For instance, in

the case of water the well profile is at a high temperature almost rectangular ($f \approx 0.9$ at 81.4 °C), whereas at low temperature it resembles a parabolic profile ($f \approx 0.65$ at -5.6 °C). In the case of ice the well becomes almost parabolic ($f \approx 0.15$).

The form factor f accounts implicitly for the influence on the spectrum of collisions of librating dipoles with surrounding medium. The stronger are the interactions in a liquid, the less is the fitted form factor f , i.e., the more the potential profile declines from the rectangular one. Unspecific interactions, characteristic for nonassociated liquids, resemble frequency dependences typical for liquid water. If one is to apply the hat model for calculation of the absorption spectrum, then the main distinctions between nonassociated and associated (water) fluids become as follows. In the first medium (e.g., CH_3F) (i) the number of the reorientation cycles performed by a permanent dipole during the lifetime of the hat potential is much shorter than in the case of water, thus indicating that molecular rotation is more damped and chaotic than in associated liquids; (ii) absence of specific interactions (and correspondingly of the translational band) arising due to H-bonding of the molecules; (iii) the greater form factor: $f(\text{CH}_3\text{F}) \approx 0.96$, whereas $f(\text{H}_2\text{O}) \approx 0.8$ and $f(\text{D}_2\text{O}) \approx 0.7$. It was suggested, therefore,¹⁰ that the parameter f presents some measure of localization of intermolecular interactions, viz. of a *spread of short-range forces* in a liquid. These forces are revealed at larger distances for lower f . Roughly, this spread could be estimated as a length of the curved part $(1 - f)\beta$ of the well: $\text{spread} = (1 - f)\beta r_{\text{mol}}$, where r_{mol} is the mean radius of a reorienting molecule. At room temperature one can take for H_2O $\beta = 21.5^\circ$, $f = 0.7$, $r_{\text{mol}} \approx 1.5$ Å; then $\text{spread} \approx 0.12$ Å. For D_2O an analogous estimate gives $\text{spread} \approx 0.2$ Å, whereas for ice the spread is as much as ≈ 0.5 Å. Hence, the short-range interactions become more enhanced in the sequence: light water \rightarrow heavy water \rightarrow ice. Note in contrast that, in such a simple nonassociated liquid, as CH_3F , we have¹⁰ $f = 0.96$, $\beta = 22.9^\circ$, $r_{\text{mol}} \approx 3.9$ Å, so that an almost rectangular intermolecular well corresponds to these parameters (see ref 10, Figure 40c) characterized by a very small spread (≈ 0.03 Å).

The equation of motion of a reorienting dipole, governed by the hat potential, is nonlinear, so the law of a periodic libration is rich in high harmonics, especially at high temperature. Due to a nonlinear equation of motion, the form of the librational band is far from being Lorentzian.

In Figure 1a we depict the contribution of librations to wideband loss spectrum of water calculated in terms of the hat model for room temperature (27 °C). For ice at -7 °C a similar calculation gives a much narrower band, see Figure 1b. During the lifetime τ_{or} a dipole performs in water and ice about two librations and about six librations in supercooled water ($m_{\text{or}} = 5.6$).

An important feature of the LIB state (it is confirmed by experimental data) presents a strong isotopic shift of the loss-peak frequency ν_{or} . Because in the chosen potential a polar molecule librates almost freely, ν_{or} is determined by the moment of inertia $I_{\text{or}}(\text{H}_2\text{O})$, which comprises about half of $I_{\text{or}}(\text{D}_2\text{O})$. Therefore, $\nu_{\text{or}}(\text{H}_2\text{O}) \approx \sqrt{2}\nu_{\text{or}}(\text{D}_2\text{O})$.

The VIB state concerns the next mechanisms, (b)–(d), which are illustrated in Figure 2, respectively, by vibrational modes 1–3.

Mechanism b: Loss Contribution ϵ''_{q} Due to Longitudinal Vibration of a Nonrigid Dipole.¹³ We consider two vibrating oppositely charged ions of water H_2O assuming that two H_2O molecules form a nonrigid $\text{O}^+ - \text{H} \cdots \text{O}^-$ dipole (other molecular groups could also be attached to the oxygen atoms). The

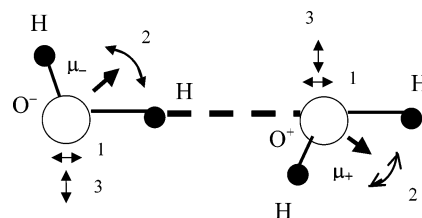


Figure 2. Scheme of the dimer of charged water molecules performing various collective vibrations: 1, longitudinal vibration of a nonrigid dipole; 2, harmonic reorientation of permanent dipoles μ^- and μ^+ ; 3, nonharmonic transverse vibration of a nonrigid dipole. Solid and dashed lines depict respectively the covalent and hydrogen bonds.

concentration N_{vib} of charged molecules is commensurable with the total concentration N of water molecules (our estimate shows that $N_{\text{vib}} \approx N/3$). A nonrigid dipole performs a longitudinal harmonic vibration governed by the elastic force constant k_{H} , fitted in such a way that the loss peak ϵ''_{q} is located in the center ν_{q} of the translational band (T-band), the frequency ν_{q} being about 200 cm^{-1} . Note, the constant k_{H} parametrizes the strained-state potential energy U in the time-varying H-bond stretch $\Delta l(t)$ via $U(k_{\text{H}}) = (1/2)k_{\text{H}}\Delta l^2$. The calculated loss curves $\epsilon''_{\text{q}}(\nu)$ are depicted in Figure 3a for water at 27 °C and in Figure 3b for ice at -7 °C. We see that the bandwidth of the loss curve $\epsilon''_{\text{q}}(\nu)$ is several times wider in water than in ice. However, in ice the frequency ν_{q} , determined by the HB elastic constant k_{H} , does not increase much. Because the equation of motion pertinent to longitudinal vibration is linear, the profile of the curve $\epsilon''_{\text{q}}(\nu)$ is Lorentzian.

In the case of water the center frequency ν_{q} is almost independent of temperature: $\nu_{\text{q}}(\text{water}) \approx 165 \text{ cm}^{-1}$; however, at room temperature $\nu_{\text{q}}(\text{water}) \approx 190 \text{ cm}^{-1}$. Such a difference in ν_{q} value perhaps indicates that a certain change of structure occurs in water at ≈ 300 K (this conclusion is supported by other facts^{15,22}). The lifetime τ_{q} is very short in the case of water: it is near 0.08 ps and slowly increases with a decrease of temperature. In ice this time is several times longer. It appears that in ice longitudinal vibration of H-bonded molecules is much less chaotic than in water. On the other hand, such vibration is much less chaotic than reorientation in defects of ice structure: Thus, $\tau_{\text{q}}(\text{ice}) \gg \tau_{\text{q}}(\text{water})$ and $\tau_{\text{q}}(\text{ice}) \gg \tau_{\text{or}}(\text{ice})$.

It appears that the H-bond is polarized. In view of our estimate, the mean moment μ_{q} of a nonrigid dipole is about 3 times larger than the moment μ_{or} of a permanent dipole librating in the hat well: $\mu_{\text{q}}/\mu_{\text{or}} \approx 7/2.5$.

Mechanism c: Loss Contribution ϵ''_{μ} Due to Harmonic Reorientation of a Permanent Dipole about the H-Bond.¹³

In a first approximation this mechanism yields, just as in mechanism b, one Lorentz line (we term it the V-band). Its center frequency ν_{μ} , located near ν_{q} , is such that usually $\nu_{\mu} < \nu_{\text{q}}$ (cf. Figure 3c with Figure 3a and also Figure 3d with Figure 3b). In terms of our approach the frequency ν_{μ} is determined by the dimensionless rotary force constant c_{rot} related to the rotational part of the strained-state potential energy as $U(c_{\text{rot}}) = (1/2)c_{\text{rot}}k_{\text{H}}l^2\theta_+^2$, where l is the mean length of the undisturbed hydrogen bond and θ_+ is a current (depending on time t) turn of the H-bond with respect to its equilibrium position. In the dimer of water molecules, used in calculations, $l = r_{\text{OO}} - r = 1.83$ Å, where $r_{\text{OO}} = 2.85$ Å is the mean distance between neighboring oxygen atoms and $r = 1.02$ Å is the covalent-bond length.

In the case of ice the T- and V-bands are resolved as separate bands (see Figure 6 below), so that the constant c_{rot} could be fitted with account of the experimental data. In the case of water

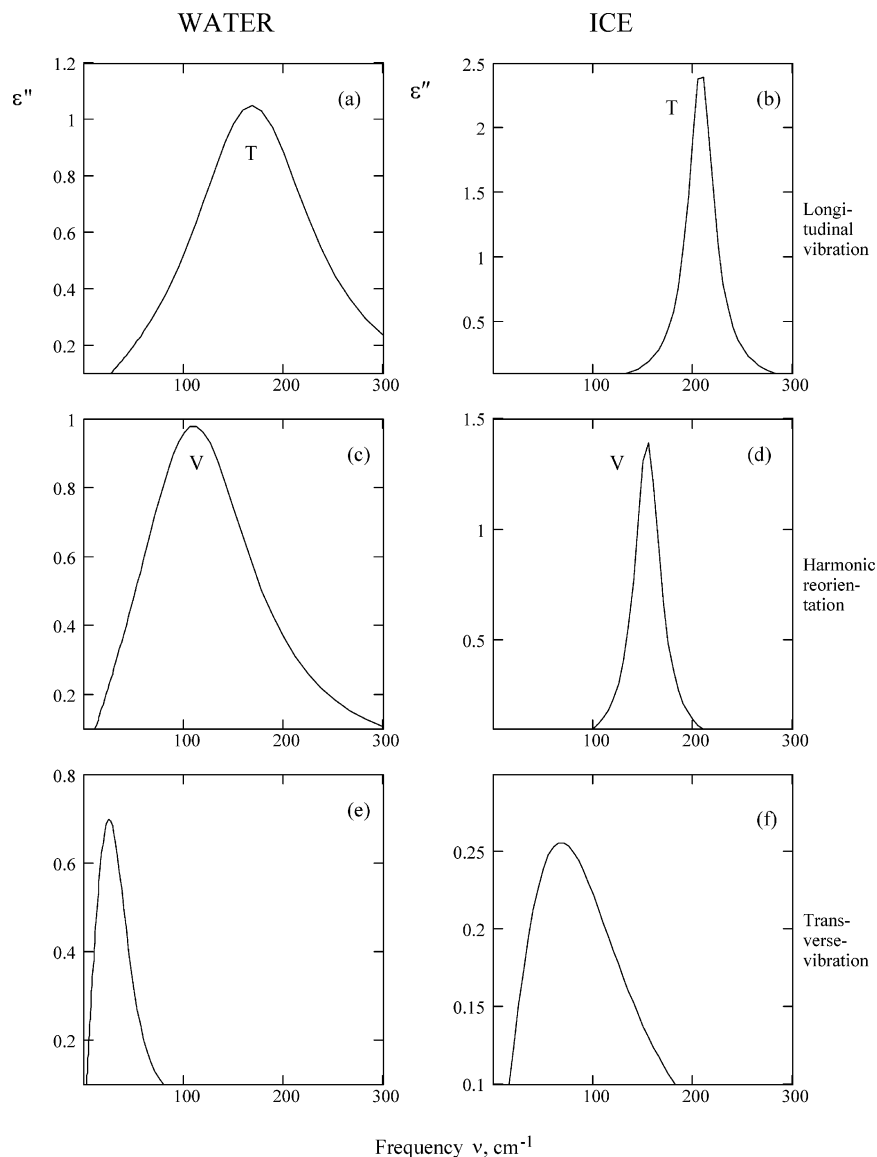


Figure 3. Contributions to the loss factor of water at 27 °C (a, c, e) and of ice at -7 °C (b, d, f) due to specific vibrations of HB molecules: (a, b) for longitudinal harmonic vibration of a nonrigid dipole; (c, d) for harmonic reorientation of a permanent dipole; (e, f) for nonharmonic transverse vibration of a nonrigid dipole. Symbols T and V refer, respectively, to the T- and V-bands.

these bands overlap (see Figure 4 below). Our studies show that $c_{\text{rot}}(\text{water})$ is close to $c_{\text{rot}}(\text{ice})$ and the rotary-vibration lifetime τ_{μ} is close to the longitudinal-vibration lifetime τ_{q} . One may regard that both times are determined by harmonic motion of the hydrogen bond. For better agreement with experiment it is useful to set $\tau_{\mu} > \tau_{\text{q}}$, as will be assumed in further calculation (Figure 6).

Mechanism d: Loss Contribution ϵ'_{μ} Due to Nonharmonic Transverse Vibration (TV) of a Nonrigid Dipole. This mechanism originates under the influence of the transverse force constant k_{\perp} from a periodic displacement of two oppositely charged water molecules in the direction transverse to the equilibrium HB direction. Parametrization of our model shows that k_{\perp} comprises about one-third of the longitudinal constant k_{\parallel} . The mean TV-vibration amplitude b is rather small: it comprises about one-third of the covalent-bond length r . Despite the smallness of b , the equation of motion, governing the $b(t)$ time dependence, is nonlinear. In terms of dimensionless variables s , φ the equation of motion takes the form¹⁴ $\ddot{s} = -2ws^3$. Here $s \equiv 2b(l+r)^{-1}$ is the transverse displacement of a water molecule from the equilibrium position, $\varphi = t/\eta_{\perp}$, so

that $\dot{s} \equiv ds/d\varphi$; the normalizing constant η_{\perp} , having dimension of time, is

$$\eta_{\perp} \equiv p_{\perp}(l+r) \sqrt{\frac{m}{4k_{\text{B}}T}} \quad (1a)$$

where m is the mass of a vibrating water molecule. The factor $w \equiv [k_{\perp}l^2(1+a)^4]/8k_{\text{B}}T$ relates dimensionless TV potential energy u_{\perp} to the deflection s as $u_{\perp} = U_{\perp}/(k_{\text{B}}T) = ws$.⁴ The effective frequency (p_{\perp}) and intensity (g_{\perp}) factors allow variation, respectively, of the position ν_{\perp} and of the TV loss-maximum intensity. The latter intensity factor connects the transverse (μ_{\perp}) and longitudinal (μ_{q}) HB dipole moments by

$$\mu_{\perp}^2 = g_{\perp} \mu_{\text{q}}^2 \quad (1b)$$

To find the contribution $\Delta\epsilon_{\perp}$ to the total complex permittivity ϵ , pertinent to the TV mechanism, we introduce the complex frequency z_{\perp} as $z_{\perp} \equiv \hat{\omega}\eta_{\perp} = x_{\perp} + iy_{\perp}$, $x_{\perp} = \omega\eta_{\perp}$, $y_{\perp} = \eta_{\perp}/\tau_{\perp}$, τ_{\perp} being the TV lifetime. Then, as follows from the theory,¹⁴

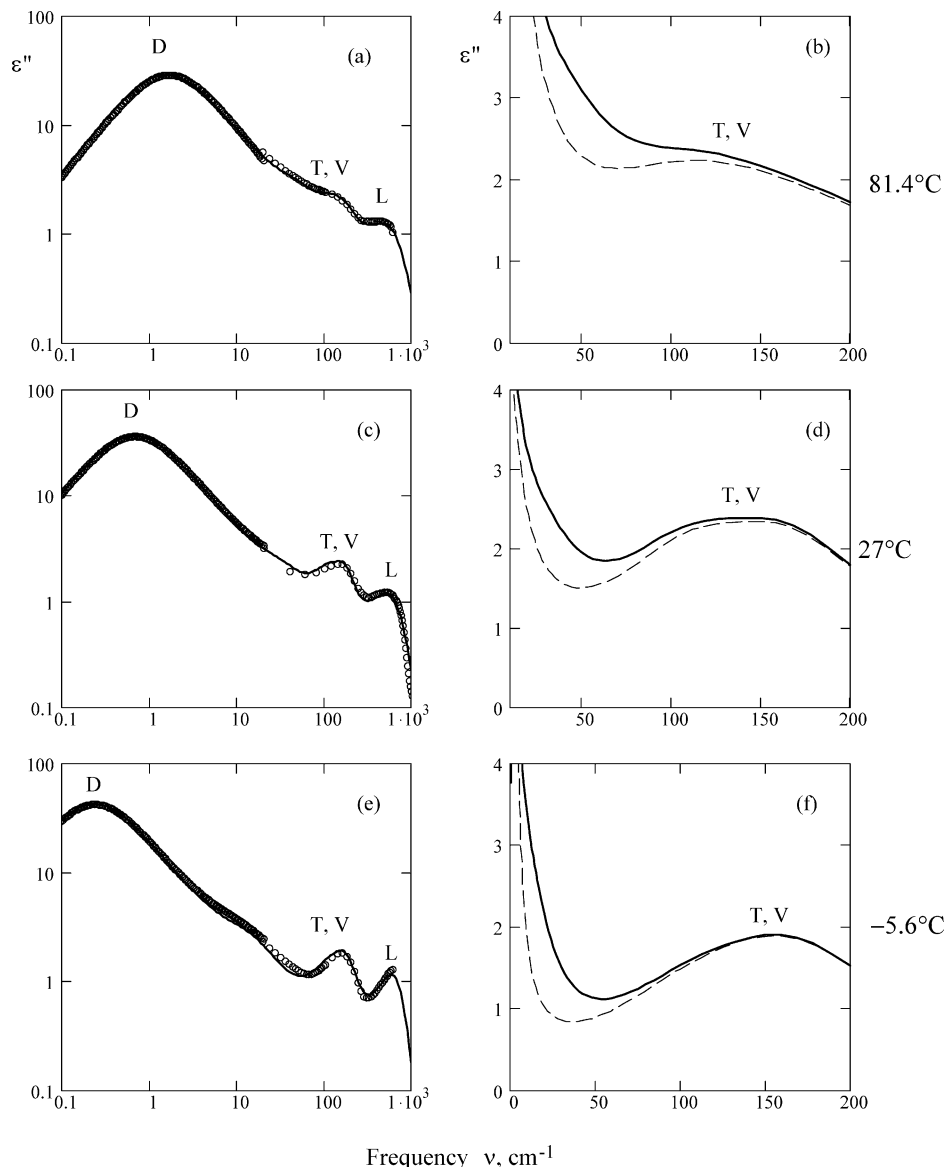


Figure 4. Dielectric loss spectra of water calculated (solid lines) and measured^{13,14} (open circles) for the temperatures 81.4° (a, b), 27° C (c, d) and -5.6° C (e, f) in a wide frequency band (a, c, d) and in the THz region (b, d, f). Dashed lines: calculation without account of transverse vibration. Symbols as in Figures 1 and 3.

$$\Delta\epsilon_{\perp} = g_{\perp} G_{\perp} L_{\perp}(z_{\perp}) \quad (2)$$

where $G_{\perp} = (\pi/k_B T)\mu_{\perp}^2 N_{\text{vib}}$ and $N_{\text{vib}} = r_{\text{vib}} N$, with r_{vib} the proportion of HB vibrating particles. The spectral function (SF) $L_{\perp}(z_{\perp})$ is found via integration over s as

$$L_{\perp}(z_{\perp}) = 3w \int_0^{s_{\text{lim}}} \frac{(18Dws^2 - z_{\perp}^2)s^6 \exp(-ws^4) ds}{12w^2s^4 + z_{\perp}^4} / \int_0^{s_{\text{lim}}} s^2 \exp(-ws^4) ds \quad (3)$$

s_{lim} being the limiting value of s , found from comparison of our theory with experiment ($s_{\text{lim}} = 0.2$). It appears that s_{lim} is in principle determined by the molecular structure.

The factor $D \equiv [2E(1/\sqrt{2})/\mathbf{K}(1/\sqrt{2})] - 1 \approx 0.627$, where $\mathbf{K}(\bullet)$ and $\mathbf{E}(\bullet)$ are the full elliptic integrals, respectively, of the first and second kind.

Calculation gives¹⁴ the following approximate formula

$$m_{\perp} \approx [1 - \exp(-u_{\text{lim}})] [8\sqrt{2}w\mathbf{K}(1/\sqrt{2})y_{\perp} \int_0^{s_{\text{lim}}} s^2 \exp(-ws^4) ds]^{-1} \quad (4)$$

for the number of vibration cycles performed by a nonrigid dipole during the lifetime $\tau_{\perp} \approx \eta_{\perp}/y_{\perp}$.

The loss frequency dependence $\epsilon''_{\perp}(\nu)$ is described by eqs 2 and 3 and is non-Lorentzian. In view of Figure 3e,f calculated, respectively, for water and ice, for reasonable dimer parameters this dependence is located in the terahertz region. Transverse vibrations are very damped, especially at low temperatures, because the parameter m_{\perp} (4) is very small. In the case of water it varies from 0.03 to 0.08, when the temperature rises from -5.6 to +81.4 °C. So low m_{\perp} values could be ascribed to collective oscillations performed by associated nonrigid dipoles. This conclusion presents a certain generalization of our model, because according to Figure 2 *formally* only two molecules participate in transverse vibration. Assuming that an *individual* dipole moment μ_{\perp}^{ind} of the transversally vibrating molecule is about that (μ_q) for the longitudinally vibrating one, we arrive at a rough estimate for an association factor ζ :

$$\zeta = \sqrt{g_{\perp}} \quad (5)$$

It follows from Table 1 that in supercooled (SC) water this factor surprisingly increases up to ≈ 12 , whereas in water at room temperature and in ice ζ is an order of magnitude less:

$$\zeta(\text{water at 300 K}) \approx 2 \quad \zeta(\text{SC water}) \approx 12.4 \\ \zeta(\text{ice}) \approx 1 \quad (6a)$$

It is very interesting that the number m_{\perp} strongly *increases* in ice:

$$m_{\perp}(\text{water at 300 K}) \approx 0.07 \quad m_{\perp}(\text{SC water}) \approx 0.03 \\ m_{\perp}(\text{ice}) \approx 1.31 \quad (6b)$$

So sharp an increase of the ratio $m_{\perp}(\text{ice})/m_{\perp}(\text{SC water})$, comprising about 20, corresponds to the decrease in ice of the association factor (as compared with that in SC water) and perhaps is somehow related to the water \rightarrow ice phase transition. Note this transition is accompanied by enhanced narrowing of the librational, translational and V-bands, cf., respectively, Figure 1b with 1a, Figure 3b with 3a, and Figure 3d with 3c.

It should be noted that comparison of frequency dependences $\epsilon''_{\perp}(\nu)$, calculated for ice and water, such as shown in (f) and (e) of Figure 3, does not permit a direct comparison of the change of ice/water dynamics, induced by the water \rightarrow ice transition, because these dependences are determined by many other parameters of the system under consideration.

Overall Loss Spectrum of Liquid Water. The total complex permittivity is found as a sum

$$\epsilon = \epsilon_{\text{or}} + \Delta\epsilon_{\text{vib}} \quad (7)$$

of contributions from molecules, reorienting in the hat well, and from vibrating HB molecules. The first term in (7) refers to permittivity of the LIB state, viz. to mechanism a, and is given by

$$\epsilon_{\text{or}} = (1/4)[12\pi\chi_{\text{or}} + n_{\infty}^2 + \sqrt{(12\pi\chi_{\text{or}} + n_{\infty}^2)^2 + 8n_{\infty}^4}] \quad (7a)$$

We employ the Gross collision model,^{8–10} for which the complex susceptibility χ_{or} is determined by the autocorrelator (“spectral function” given in refs 12 and 13) L_{or} of the hat model as

$$\chi_{\text{or}} = \frac{g_{\text{or}}G_{\text{or}}(1 - r_{\text{vib}})z_{\text{or}}L_{\text{or}}}{g_{\text{or}}\chi_{\text{or}} + iy_{\text{or}}L_{\text{or}}}$$

where the normalized concentration

$$G_{\text{or}} = \frac{\mu_{\text{or}}^2(1 - r_{\text{vib}})N}{3k_{\text{B}}T}$$

and the Kirkwood correction factor

$$g_{\text{or}} = \frac{(\epsilon_s - \Delta\epsilon_s - n_{\infty}^2)[2(\epsilon_s - \Delta\epsilon_s) + n_{\infty}^2]}{12\pi G_{\text{or}}(1 - r_{\text{vib}})(\epsilon_s - \Delta\epsilon_s)}$$

$n_{\infty}^2 \approx 1.7$ is the optical permittivity (at the end of the dielectric-relaxation region); the librating-dipole moment μ_{or} is connected with that (μ_0) of a free water molecule as $\mu_{\text{or}} = (1/3)k_{\mu}\mu_0(n_{\infty}^2 + 2)$, the fitting coefficient k_{μ} being close to unity.

The second term in (7) represents the composite complex permittivity

$$\Delta\epsilon_{\text{vib}} = \Delta\epsilon_{\text{q}} + \Delta\epsilon_{\mu} + \Delta\epsilon_{\perp} \quad (8)$$

due to mechanisms b–d. For the first two terms in (7) we employ the simplified formula, presented in ref 13 as a sum of two Lorentz lines. The analytic expression for the last term in (8) is given above by eqs 2 and 3. The symbol Δ is used in (7), because the *optical* part n_{∞}^2 of the permittivity ϵ' , not depending on frequency, is already included in the first term in (7): $\text{Re}(\Delta\epsilon_{\text{vib}}) \rightarrow 0$ at the end of the overall band under consideration. We have from (7) the vibration loss as

$$\epsilon''_{\text{vib}} = \epsilon''_{\text{q}} + \epsilon''_{\mu} + \epsilon''_{\perp} \quad (9)$$

In the above we have considered each term in (7), below we shall calculate the total loss

$$\epsilon''(\nu) = \epsilon''_{\text{or}} + \epsilon''_{\text{vib}} = \epsilon''_{\text{or}} + \epsilon''_{\text{q}} + \epsilon''_{\mu} + \epsilon''_{\perp} \quad (10)$$

In Figure 4a,c we show by solid lines the loss spectrum $\epsilon''(\nu)$ calculated in the wide band 0.1–1000 cm^{-1} for the temperatures 81.4 and 27 °C. The experimental frequency dependences, depicted by open circles, are taken from ref 23 for 27 °C and ref 24 for 81.4 °C.

The curves in Figure 4b,d marked by solid lines concern the narrower terahertz region and describe the specific phenomena related to vibration of HB molecules. The calculation, not accounting for the TV vibration, is depicted in Figure 4b,d by dashed lines. It is evident that the transverse vibration plays a noticeable role. In this region a certain loss “deficit” is characteristic. The seeming impossibility to overcome this deficit theoretically was one of the main problems of our early investigations.¹⁰

The loss peak located near frequency 150 cm^{-1} (it is depicted as T, V) originates from harmonic elastic vibration of HB molecules. The minimum in the T, V curves at $\sim 50 \text{ cm}^{-1}$ gets washed out with increase of T : at high temperature the curve $\epsilon''(\nu)$ decreases monotonically (Figure 4a,b). Note, the fitted proportion r_{vib} of vibrating HB molecules undergoes with change of T only small changes. We see that the T- and V-bands are barely separated in the case of water, where usually they are both jointly called “translational band”.

The loss peak near the border of the far-IR region, at $\nu \approx 700 \text{ cm}^{-1}$, depicted as L, arises due to reorientation of a rigid dipole in the hat well. This mechanism is responsible also for a rather wide microwave loss peak, depicted as D, which is located between the frequencies 0.1 and 10 cm^{-1} . In this region and at lower frequencies our theory is parametrized with account of the empirical analytical formula¹⁷ for ϵ to obtain agreement of the calculated complex permittivity ϵ with that given by Debye theory. Our parametrization also shows, in agreement with known experimental data and the results^{15,22} of modeling of dielectric spectra, that a monotonic dependence on T of some fitted model parameters experiences a break at room temperatures. This phenomenon perhaps indicates that a certain structural change occurs in a narrow temperature interval near 300 K.

The calculated spectrum (Figure 4a,c) agrees very well with experiment.^{23,24} However, we should state the reservation that a certain scattering is observed in these measurements.

Wideband Loss Spectrum of Supercooled (SC) Water. For this calculation the same formulas were used as those employed in the previous section. This spectrum is depicted in Figure 4e,f, which concerns $-5.6 \text{ }^{\circ}\text{C}$. For all temperatures the same hat-potential value U_{or} is retained. The other fitted parameters are also retained or changed a little, with the following exceptions

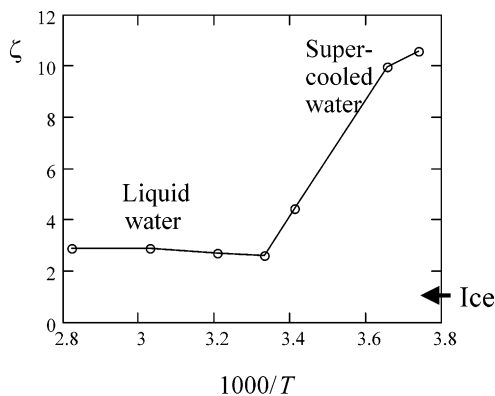


Figure 5. Temperature dependence of the association factor (5).

(see Table 1): (i) the effective frequency and intensity parameters p_{\perp} and g_{\perp} introduced, respectively, in (1a) and (1b), substantially increase; (ii) the lifetime τ_{or} , viz. lifetime of the hat potential, approximately doubles.

Transition from +27 to -5.6 °C reveals itself in (a) increase of the “loss deficit” (of space between the solid and dashed curves in Figure 4d,f), (b) the low-frequency shift of the TV loss maximum, and (c) decrease of the TV-lifetime τ_{\perp} . Increase of p_{\perp} and g_{\perp} at $T = -5.6$ °C (as compared with their values at 27 °C) confirms the above statement that *association of molecules increases in water at low temperatures*. In Figure 5 we represent the temperature dependence of the association factor ζ introduced by eq 5. This dependence exhibits a very sharp increase of ζ with a decrease of T for $T < 300$ K. This increase means that the fitted “longitudinal” dipole moment μ_{\parallel} remains practically constant with a decrease of temperature, whereas the “transverse” moment μ_{\perp} drastically increases. The association factor ζ is in SC water about 6 times greater than in water at room temperature. So, our results mean that more than two molecules may participate in collective motion and that this effect reveals itself in SC water in the THz region 1–100 cm^{-1} .

Note, in terms of our semiphenomenological approach the first mention of collective molecular motions, given in ref 13, is actually supported by the $\zeta(T)$ sharp rise (Figure 5), whereas previously¹⁰ only gas-like models were employed in our works, in which molecular association was neglected. Perhaps, one may consider this phenomenon as a feature relating to the water \rightarrow ice transition. Therefore, the use for calculation of a dimer depicted in Figure 2 becomes rather conditional. Nevertheless, our TV model still provides an important insight into molecular interactions, if the fitting parameters p_{\perp} and g_{\perp} are regarded as those giving a semiphenomenological description of the far-IR spectra in the fluid under consideration.

The librational band narrows (cf. Figure 4c,e) in supercooled water, the frequency ν_{or} of its maximum lowers; and the absorption band near the frequency 150 cm^{-1} is revealed more distinctly than at room temperature (cf. Figure 4d,f). One might suppose that similar consideration could also be useful regarding physical processes in glasses and biological objects.

Resonance Far-Infrared Spectrum of Ice. We consider the ice H_2O spectrum at the temperature -7 °C in the frequency range 10–1000 cm^{-1} . In comparison with the two previous sections, related to water, the calculation scheme is modified as follows:

(i) The high-frequency approximation^{12,13} is used also for the LIB state, viz. also for molecules reorienting in the hat well. Instead of (7a), the complex permittivity of this state is represented as

$$\epsilon_{\text{or}} \approx \Delta\epsilon_{\text{or}} + \delta_{\infty} \quad \Delta\epsilon_{\text{or}} = 6\pi L_{\text{or}}(z_{\text{or}}) \quad (11)$$

so that the total complex permittivity is calculated from the expression

$$\epsilon \approx \epsilon_{\text{or}} + \Delta\epsilon_{\text{vib}} = \Delta\epsilon_{\text{or}} + \Delta\epsilon_{\text{vib}} + \delta_{\infty} \quad (12)$$

The constant δ_{∞} is obtained from the condition that the total dielectric constant $\text{Re}[\epsilon(\nu)]$, found from (12), should at its minimum (near the end of the far-IR region) slightly exceed unity. In our calculation δ_{∞} is close to the optical permittivity n_{∞}^2 : $\delta_{\infty} = 1.9$, whereas $n_{\infty}^2 = 1.7$.

(ii) For two elastically vibrating HB molecules we employ, as was mentioned above, two slightly different lifetimes τ_{q} and τ_{μ} (above we set $\tau_{\mu} = \tau_{\text{q}} \approx \tau_{\text{vib}} \approx 0.08$ ps, whereas in this calculation $\tau_{\text{q}} \approx 0.23$ ps and $\tau_{\mu} \approx 0.34$ ps). This yields better agreement with the experiment.²⁵

The resulting far-IR absorption (a) and loss (b) spectra are presented for ice in Figure 6 (several fitted/estimated parameters are given in Table 1). The calculated spectrum, shown by solid lines, agrees better with the experimental spectrum,²⁵ depicted by open circles, than the spectra obtained previously¹³ without improvement (ii) and without account of the last term in (10). Although, as seen from Figure 6, the $\epsilon''_{\perp}(\nu)$ dependence, depicted by dashed curve, is low (it is rather close to the abscissa axis), the role of transverse vibration is, however, fundamental, especially, in respect of the ice THz spectrum. We also see from Figure 6 that the T- and V-bands (depicted by the symbols T and V) unlike water are resolved. This circumstance ultimately justifies involving the harmonic “reorientation” mechanism (c) along with the harmonic “longitudinal” mechanism (b).

Conclusions. Consideration of transverse vibration of HB molecules, supplemented by description of mechanisms a–c, facilitates a *quantitative* agreement between the calculated far-infrared water/ice and experimental^{17,23–25} spectra. Such an agreement, reached after parametrization of the employed model, could not be obtained previously^{13,22}—neither for ice and supercooled water nor for liquid water at temperatures near the boiling point.

It seems on the face of it that it is possible to successfully describe analytically the spectrum of a fluid, containing several absorption/loss peaks, with the concomitant large number of free parameters. Actually, however, it is hardly possible. *For ice* we do not know any attempt of such sort. *For water* most attempts were made for the relaxation (Debye) spectrum containing a single loss peak ϵ'' in the microwave region. In a pioneering work¹⁷ by Liebe et al. an explanation of the wideband water spectrum $\epsilon(\nu)$ was given in terms of two Debye and two Lorentz lines (see also ref 10, p 144, and ref 15). Unfortunately, this representation is not applicable for the temperatures exceeding the room temperature;¹⁵ moreover, it does not allow us to *interpret* the influence of temperature on water spectra. On the contrary, our description allows a coherent interpretation of the change of water spectra in a wide temperature range¹⁵ as well as the comparison (in terms of the same model) of parameters employed for water, supercooled water and ice.

In the first part of this article we have analyzed the spectrum provided by each of four mechanisms, and in the second part we have calculated the overall loss spectra (10) and (12), respectively, for water and ice. Our approach gives a correct description of the main features of these spectra, which in the far-IR range exhibit several maxima and minima with specific temperature dependences. These results are achieved by considering (a) libration of a rigid dipole in the hat potential, (b) elastic harmonic vibration of a nonrigid dipole along the H-bond,

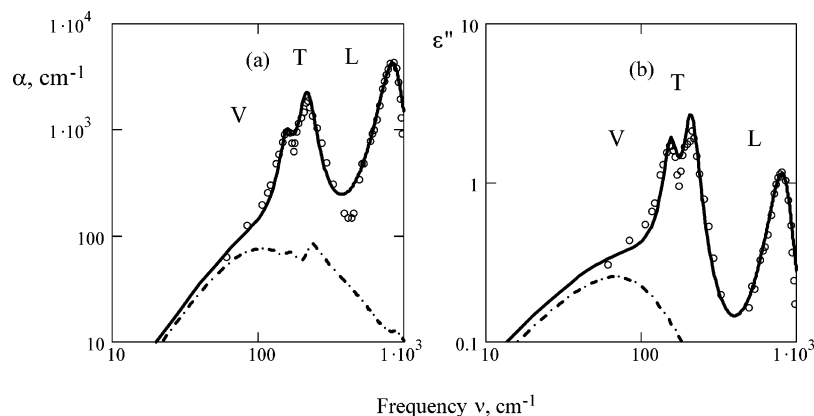


Figure 6. Absorption (a) and loss (b) spectra of ice calculated at the temperature $-7\text{ }^{\circ}\text{C}$ (solid lines); dashed lines, calculation of absorption (a) and loss (b) generated by transverse vibration; open circles, experimental data.²⁵

(c) elastic harmonic reorientation of a rigid dipole about such a bond, and (d) nonharmonic bending vibration of a nonrigid dipole perpendicular to the H-bond.

A simple formula (5) is proposed for an association factor ζ relating the dipole moments μ_{\perp} and μ_{\parallel} of transversally and longitudinally vibrating molecules. In view of Figure 5 it follows from our theory, parametrized with account of terahertz water spectra, that the sharp rise of this factor ζ should occur, if the temperature decreases below 300 K. However, in ice this factor drops by an order of magnitude: $\zeta(\text{SC water}) \approx 12.4$, whereas $\zeta(\text{ice}) \approx 1$. Therefore, the factor ζ represents some characteristic of structural/phase transitions occurring in aqueous fluids with change of temperature. Note that on the other hand the neutron diffraction reveals²⁶ some similarity between deeply cooled water and different forms of ice.

It appears that the MD simulation method, which is in principle more fundamental than the employed semiphenomenological (SP) approach, up to now yields¹⁻⁷ only a *qualitative* agreement of theory with experiment. Such an advantage of the SP modeling arises, in our opinion, mainly due to following reason. Our autocorrelator (the spectral function $L(z)$), which is linearly related to the dipolar ACF spectrum) involves⁸⁻¹⁰ distribution over *times* t_{ν} between strong collisions of dipoles. The mean value τ of these times, termed simply “lifetime”, represents an important parameter of our theory. Indeed, the complex spectral function $L(z)$ is represented as $L(\omega\eta + i\eta/\tau)$, where ω is the angular frequency of radiation and η is the microscopic parameter of the type (1a) having the dimension of time. In the SP approach we introduce four lifetimes τ_{or} , τ_{q} , $\tau_{\mu} \approx \tau_{\text{q}}$, and τ_{\perp} , corresponding, respectively, to the motion types a–d. *These lifetimes are fitted* (see Table 1) to get the best agreement with the experimental spectra, whereas in a typical MD calculation scheme (see, e.g., ref 6) a similar fitting procedure is lacking, because only a few *steady-state* water parameters are involved, and therefore there is no means for allowing fine adjustment of the MD-calculated spectrum.

We may provide the following facts giving an independent support of our model/theory.

(1) The angle 2β , through which a permanent dipole turns in the hat well, and the corresponding linear displacement L , agree with the data.^{19,27}

(2) The fitted lifetimes τ of fast molecular motions, commensurable with a part of a picosecond, have the same order of magnitude as, e.g., in the work.²⁸

(3) The dimer’s dimensions correspond to the accepted standard.

(4) The employed concept that the translational band, placed near 180 cm^{-1} , is determined mainly by movements of oxygen atoms is widely spread; see, e.g., ref 29.

(5) Mechanism d of nonharmonic transverse vibration was successfully applied³⁰ for calculation of nonresonance ice spectra in the submillimeter wavelength range.

In the future it would be desirable to apply the semiphenomenological approach for the following:

(i) Analytical calculation, in a range of temperatures, of resonance and nonresonance ice spectra, including the low frequency relaxation band. Note, only empirical descriptions of nonresonance ice spectra are known (see, e.g., ref 18), some exception being the work.³¹ An incorrect interpretation of the origin of the ice relaxation spectrum may be found in the literature (see, e.g., ref 21).

(ii) Elaboration of the theory allowing calculation of the low-frequency Raman scattering spectra in terms the same model that is used for our study of dielectric spectra of water and ice.

Note Added in Proof. In recent work³² it was shown in terms of the first-principle quantum approach that for a tetrahedral coordination of O atoms the polarization effects depend on the environment, unlike previous MD calculation, in a strong *intermolecular* way. Our simplified classical approach, in which the translational band is ascribed to interaction of two adjacent *charged* molecules, qualitatively agrees with ref 32, since we actually ascribe this band to the same origin.

Acknowledgment. We are grateful to M. N. Rodnikova, A. Yu. Zasetski, J. Teixeira, G. G. Malenkov and I. N. Kochnev for helpful discussion. V.G. acknowledges the hospitality of Prof. W. T. Coffey in Dublin and financial support of Trinity College Dublin.

References and Notes

- (1) Nielson, G.; Townsend, R. M.; Rice, S. A. *J. Chem. Phys.* **1984**, *81*, 5288.
- (2) Marchi, M. *J. Chem. Phys.* **1986**, *85*, 2414.
- (3) Guillot, B. *J. Chem. Phys.* **1991**, *95*, 1543.
- (4) Silvestrelli, P. L.; Bernasconi, M.; Parrinello, M. *Chem. Phys. Lett.* **1997**, *277*, 478.
- (5) Bursulaya, B.; Kim, H. J. *J. Chem. Phys.* **1998**, *109*, 4911.
- (6) Zasetsky, A. Yu.; Khalizov, A. F.; Sloan, J. J. *J. Chem. Phys.* **2004**, *121*, 6941.
- (7) Zasetsky, A. Yu.; Khalizov, A. F.; Earle, M. E.; Sloan, J. J. *J. Phys. Chem.* **2005**, *109*, 2760.
- (8) Gaiduk, V. I.; Tseitlin, B. M. *Adv. Chem. Phys.* **1994**, *87*, 125–378.
- (9) Gaiduk, V. I. *Dielectric Relaxation and Dynamics of Polar Molecules*; World Scientific: Singapore, 1999.

- (10) Gaiduk, V. I.; Tseitlin, B. M. *Adv. Chem. Phys.* **2003**, *127*, 65–331.
- (11) Gaiduk, V. I.; Tseitlin, B. M.; Crothers, D. S. F. *J. Mol. Liq.* **2004**, *114*, 63.
- (12) Gaiduk, V. I.; M Tseitlin, B.; Crothers, D. S. F. *J. Mol. Struct.* **2005**, *738*, 117.
- (13) Tseitlin, B. M.; Gaiduk, V. I.; Nikitov, S. A. *J. Commun. Technol. Electron.* **2005**, *50*, 1085–1106.
- (14) Gaiduk, V. I.; Crothers, D. S. F. *J. Mol. Liq.*, in press.
- (15) Gaiduk, V. I.; Crothers, D. S. F. *J. Mol. Struct.*, in press.
- (16) Agmon, N. *J. Phys. Chem.* **1996**, *100*, 1072.
- (17) Liebe, H. J.; A Hufford, G.; Manabe, T. *Intl. Infrared, J.; Millimeter Waves* **1991**, *12*, 659.
- (18) Hufford, G. *Intl. Infrared, J.; Millimeter Waves* **1991**, *12*, 677.
- (19) Teixeira, J. Bellissent-Funel, M.-C.; Chen, S. H.; Dianoux, A. J. *Phys. Rev. A* **1985**, *31*, 1913.
- (20) Teixeira, J. Private communication, 2005.
- (21) Maeno, N. *Science About Ice*; MIR: Moscow, 1988 (in Russian, translation from Japanese).
- (22) Gaiduk, V. I.; Nikitov, S. A. *Opt. Spectrosc.* **2005**, *98*, 919.
- (23) Downing, H. D.; Williams, D. *J. Geophys. Res.* **1975**, *80*, 1656.
- (24) Zelsmann, H. R. *J. Mol. Struct.* **1995**, *350*, 95.
- (25) Warren, G. S. *Appl. Opt.* **1984**, *23*, 1206.
- (26) Bellissent-Funel, M.-C.; Bosio, L. *J. Chem. Phys.* **1995**, *102*, 3727.
- Bellissent-Funel, M.-C. *Il Nuovo Chimento* **1998**, *20 D*, 2107.
- (27) Bratos, S.; Diraison, M.; Tarjus, G.; Leiknam, J.-Cl. *Phys. Rev. A* **1992**, *45*, 5556.
- (28) Bertolini, D.; Cassettari, M.; Ferrario, M.; Grigolini, P.; Salvetti, G. *Adv. Chem. Phys.* **1985**, *62*, 277.
- (29) Nielsen, O. F.; Johansson, C.; Jakobsen, K. L.; Christensen, D. H.; Wiegell, M. R.; Pedersen, T.; Gniadecka, M.; Wulf, H. C.; Westh, P. *Proc. SPIE* **2000**, *4098*, 160.
- (30) Gaiduk, V. I.; Kutuza, B. G. *Opt. Spectrosc.*, in press.
- (31) Golunov, V. A.; Korotkov, V. A.; Sukhonin, E. V. *Overall Results of Science and Technique*; Radio Engineering Series; VINITI: Moscow, 1990; Vol. 41, p 68 (in Russian).
- (32) Sharma, M.; Resta, R.; Car, R. *Phys. Rev. Lett.* **2005**, *95*, 187401.